

Lymphoma in Psittacine Birds: A Histological and Immunohistochemical Assessment

Daniel J. Gibson¹ , Nicole M. Nemeth², Hugues Beaufrère¹ , Csaba Varga^{1,3} , Michael M. Garner⁴, and Leonardo Susta¹ 

Veterinary Pathology
2021, Vol. 58(4) 663-673
© The Author(s) 2021



Article reuse guidelines:
sagepub.com/journals-permissions
DOI: 10.1177/03009858211002180
journals.sagepub.com/home/vet



Abstract

In psittacine birds, round cell neoplasms that originate from lymphocytes, plasma cells, histiocytes, or mast cells are sporadic and poorly described. The lack of morphological and immunohistochemical diagnostic criteria or grading schemes make specific diagnoses and prognoses challenging. We assessed cases of psittacine birds diagnosed with round cell neoplasia from 3 North American veterinary diagnostic laboratories to describe the diagnostic features of these tumors. For all cases, demographic data, anatomic distribution, histological features, and immunoreactivity for T (CD3) and B (Pax5 and MUM-1) cell markers were assessed using tissue microarrays and whole slide mounts. Thirty-eight psittacine birds representing 14 species were included. Tumors were mainly infiltrative and multicentric, were composed of homogenous sheets of round to polygonal cells, and commonly presented with a high mitotic count (average 21 mitoses per high-power field). Based on Pax5 immunoreactivity, B-cell lymphoma was most common (19/38 [50%]), and was significantly associated with involvement of the gastrointestinal and urogenital systems. Of the 38 cases, 6 (16%) were consistent with T-cell lymphoma, 3 (8%) with plasma cell tumor, and 3 (8%) were double-reactive for both B- and T-lymphocyte markers. This is the first study to describe morphologic and immunohistochemical features of round cell neoplasia in a large number of psittacine birds, and provides benchmark data for future studies aimed at elucidating the diagnosis and prognosis of these neoplasms. These data also provide useful information about reactivity of commercially available antibodies as lymphocyte markers in tissues of multiple psittacine species.

Keywords

lymphoma, round cell neoplasia, histopathology, immunohistochemistry, immunophenotype, *Psittaciformes*, avian

In veterinary medicine, round cell neoplasia is a broad term that encompasses tumors with round cell morphology, including lymphoma, histiocytic neoplasms, plasma cell tumor, and mast cell tumor, which can be difficult to differentiate based solely on histopathology. Lymphoma is the most common type of round cell neoplasia in psittacine birds,^{5,14} and unlike lymphoid neoplasia in several other avian species (ie, poultry),³ no evidence for a viral etiology has been identified. Similar to other neoplastic diseases, older psittacines are most affected,⁵ and existing literature suggests that lymphoma in these species has a high mortality rate, with only 1 report describing a curative treatment.¹⁷ Assessment of a large case series summarizing features of lymphoma in a variety of pet bird species revealed that the most commonly affected organs were liver, spleen, and kidney (in descending order of frequency);⁵ however, there are no published data that specifically describe common features of psittacine lymphoma, and this limits the ability to accurately diagnose and classify lymphoma and other round cell tumors in these species.

Immunohistochemistry (IHC) is often necessary to diagnose a specific type of round cell neoplasia, and it is extensively used in diagnostic pathology of mammals using formalin-fixed

paraffin-embedded (FFPE) tissues. Published case reports suggest that some IHC markers commonly employed in mammalian species have diagnostic utility in psittacine birds; however, limited data on cross-reactivity of psittacine antigens with antibodies raised against the mammalian homologues is the main hurdle for application of IHC panels. Therefore, it is challenging to diagnose round cell neoplasia in birds and more specifically in psittacines. CD3 (cluster of differentiation 3) is part of the T-cell receptor and is used as a T-cell marker with cross-reactivity in psittacine FFPE tissues using antibodies for the mammalian homolog, allowing accurate diagnosis of T-cell

¹University of Guelph, Guelph, Ontario, Canada

²University of Georgia, Athens, GA, USA

³University of Illinois, Urbana, IL, USA

⁴Northwest ZooPath, Monroe, WA, USA

Supplemental material for this article is available online.

Corresponding Author:

Leonardo Susta, Department of Pathobiology, Ontario Veterinary College, University of Guelph, Guelph, Ontario, Canada N1G 2W1.

Email: lsusta@uoguelph.ca

lymphoma in psittacine species.^{11,27} In contrast, very few antibodies directed against mammalian B-cell markers are convincingly cross-reactive in psittacine FFPE tissues. Studies using antibodies raised against mammalian CD79, BLA36 (B-lymphocyte antigen 36), and CD20 antigens report inconsistent or conclusively negative immunoreactivity, indicating unsuitability of these markers in psittacine species when using routine IHC procedures.^{12,17,18,22} The Pax5 antigen is considered a pan B-cell marker in mammalian species,²⁶ and antibodies raised against the mammalian homologues have been reported to cross-react in avian FFPE tissues.^{6,21,24} In psittacines, cross-reactivity has been reported in a Pacific parrotlet (*Forpus coelestis*) diagnosed with an infiltrative orbital B-cell lymphoma.¹⁶ Similarly, MUM-1 (multiple myeloma 1), a transcription factor associated with B-cell differentiation (especially terminally differentiated B-cells),⁷ was successfully detected in FFPE samples of lymphoma in a yellow-collared macaw (*Primolius auricollis*) using an antibody against the human homologue.¹² In humans, MUM-1 expression has been demonstrated in normal germinal center B-lymphocytes, as well as in a small subset of activated T-cells; however, expression is primarily in plasma cells with nuclear and occasional cytoplasmic reactivity.⁷ Taken together, these data suggest that MUM-1 may be effective to diagnose B-cell lymphoma and plasma cell tumors in psittacine birds.

To validate the suitability of cellular markers for IHC in a new species, ideally antibody cross-reactivity should be demonstrated in large numbers of independent samples; tissue microarray (TMA) technology is useful for simultaneous assessment of numerous samples from different cases. One study used TMAs to determine the subtypes of lymphoma in ferrets and concluded that duplicate 1-mm cores were sufficient to characterize the immunophenotype of the tumors using CD3, CD79, and Ki67 markers,⁹ indicating that a diagnosis could be reached despite the small core size. Given the lack of information regarding IHC markers in exotic animals, the use of TMAs can expedite the validation of antibody cross-reactivity by including more diseased and normal control tissues into fewer cassettes.

The purpose of this case series was to describe the anatomic and histologic features of select cases of round cell neoplasia in psittacine species and to determine the corresponding immunophenotype as determined by CD3, Pax5, and MUM-1 markers through the assessment of cross-reactivity of commercially available antibodies.

Materials and Methods

Case Selection and Histology Review

Selected postmortem cases with a final diagnosis of lymphoma or round cell neoplasia from psittacine birds submitted to the Ontario Veterinary College Teaching Hospital between 1999 and 2018 were included based on availability of histologic material ($n = 13$), and compiled with cases opportunistically collected from 2 additional North American veterinary

diagnostic laboratories: Northwest ZooPath (NWZP; $n = 22$) and Université de Montréal ($n = 4$). Cases of myeloproliferative disease were not included and only non-CITES listed psittacine birds were included from the NWZP archive.

From the pathology reports of each case, data were extracted on species, sex, age, and diagnosis. Age was divided into 4 categories (ie, senior, adult, juvenile, and unknown), as described previously.⁸ Histology slides for each case were collected and reassessed at the University of Guelph by 2 investigators (DG and LS) in order to evaluate body systems and specific organs affected by the tumor, growth pattern, cellular and nuclear morphology, presence of necrosis, and mitotic count. In some cases ($n = 13$), archived material (slides or paraffin blocks) was only available from limited tissues, and therefore anatomic distribution of the tumor was assessed according to the postmortem reports. The mitotic count was the number of mitoses per $40\times$ objective field (0.34 mm^2), based on the average of 3 fields²⁶ (BX53 Olympus microscope model# U-SDO3). The mitotic counts were divided into 4 tiers: 0 to 9.9, 10 to 19.9, 20 to 39.9, and ≥ 40 mitoses/field to equally represent the ranges in the present cases. Size of neoplastic cells was categorized relative to the size of an avian red blood cell. Small cells were up to the length (approximately $12\text{ }\mu\text{m}$) of one red blood cell, medium cells were 1 to $1.5\times$ the length of a red blood cell, and large cells were $2\times$ or more the length of a red blood cell.

Tissue Microarray Construction

Tissue microarrays from neoplastic tissues were constructed to test multiple cases simultaneously for IHC (see below). The TMA cassettes were created using a TMArrayer (Pathology Devices) using triplicate 1-mm cores from paraffin blocks of each case. Cores were taken from representative areas of the tumor that did not contain extensive necrosis or autolysis, as assessed by initial case review. Tissue cores from spleen with neoplastic infiltrates were avoided, when possible, to prevent potential ambiguity when distinguishing neoplastic and non-neoplastic lymphocytes.

To assess the immunohistochemical cross-reactivity of antibodies in tissues of each psittacine species in the disease group, cores of histologically normal lymphoid organs (ie, bursa, spleen, and thymus) from 3 different conspecific birds (or congeneric, if not available) were included in the same TMA. Tissues from the closely related genus *Ara* were used for the genus *Primolius* due to lack of available congeneric tissues for this genus. Additionally, technical positive control cores were included in all TMAs and consisted of normal bursa, spleen, and thymus of a broiler chicken (on which the IHC technique for the markers was initially optimized) and canine lymph node tissue. Tumor and normal tissue cores were randomized using a random number generator within each TMA to decrease any bias due to positioning. Position number 1 was indicated by a star-shaped arrangement of extra cores to prevent loss of orientation during slide preparation.

Immunohistochemistry

To detect T and B lymphocytes, IHC for CD3, Pax5, and MUM-1 were carried out on the TMAs. IHC for CD3 was performed using a 1:400 dilution of a rabbit polyclonal antibody raised against the human homologue (Dako), and applied for 32 minutes using a Ventana autostainer platform with in-line heat-induced epitope retrieval (HIER; 30 minutes at 90 °C at pH 8) and an alkaline phosphatase-linked polymer detection system coupled with Fast Red chromogen (Ventana).

For Pax5, IHC was conducted using a mouse monoclonal antibody raised against the human homologue (clone 24/Pax5, BD Biosciences), which was applied at 1:100 dilution in background-reducing diluent (Dako) for 30 minutes. HIER was carried out for 30 minutes at 110 °C in citrate buffer (pH 6; Dako) in a decloaker. Reaction was visualized using the EnVision FLEX HRP detection system (Dako) coupled with 3,3'-diaminobenzidine (DAB) chromogen (Dako).

For MUM-1, IHC was performed using a mouse monoclonal antibody raised against the human homologue (clone MUM1p, Dako), which was applied at 1:50 dilution for 30 minutes, following HIER at pH 9 in decloaker (Biocare Medical) for 20 minutes at 97 °C. Reaction was visualized using a peroxidase-linked polymer detection system (EnVision FLEX HRP, Dako) coupled with NovaRed chromogen.

Negative technical controls for CD3 were conducted using nonimmune rabbit serum in place of the primary antibody, and were run for all tested slides. Mouse monoclonal antibodies raised against caprine arthritis-encephalitis virus (IgG1) and bovine uroplakin (IgG1) were used as isotype controls for Pax5 and MUM-1, respectively, using the same concentration of the test antibodies. These isotype controls were run in both chicken and budgerigar tissues during the IHC optimization process; however, negative technical controls for Pax5 and MUM-1 for the entire psittacine cohort were performed by excluding the primary antibody only.

Immunoreactivity Assessment

Antibody reactivity was considered successful for one species, if conspecific (or congeneric, see above) normal lymphoid tissues had the expected histological distribution of B or T lymphocytes. Internal controls (ie, normal B or T lymphocytes in the cores with neoplasia) were also assessed to verify possible lack of reactivity in neoplastic cells specific to that core or tissue; however, these were available opportunistically and could only be assessed in a few cases. Only results from cases with verified controls were further assessed.

Immunoreactivity for the disease cohort was assessed by blinded, sequential assessment of the randomized tissue cores to reduce assessment bias. If reactivity was ambiguous or insufficient tissue area remained due to core loss, assessments were made on whole mounts for all IHC markers, over the entire tumor area (ie, the original tissue block).

Reactivity for all markers was qualitatively assessed by noting the localization of reactivity within the cell (membranous, cytoplasmic, nuclear) across the available tissue area, to identify specific immunoreactivity. Then, the percent of these positive cells within the neoplastic population was visually estimated for each of the 3 markers.

Ancillary Tests

Additional testing was conducted in 3 cases (cases 29–31) using real-time polymerase chain reaction (PCR) assays to detect avian *Coxiella sp.* and *Chlamydia psittaci*. Tests were performed by the Animal Health Laboratory (AHL) at the University of Guelph, an American Association of Veterinary Laboratory Diagnosticians (AAVLD) accredited laboratory.

Statistical Assessment

To assess if specific organs or body systems (eg, gastrointestinal, hepatic) were more likely to be affected by specific tumors, linear regression was performed using the percent of immunoreactive cells for each marker as the outcome (dependent) variable. Each of the 3 markers were assessed independently as continuous variables and regressed in individual models using a single body system or organ (binary variable) as the predictor (independent) variable. The simple linear regression equation can be described as $Y = \beta_0 + \beta_1 X$, where Y is the outcome variable, X is the predictor variable, β_0 is the value of the outcome variable Y when the predictor variable X equals zero, and β_1 is the estimated regression coefficient that quantifies the association between the predictor variable X and the outcome variable Y .

Body systems that had significant regression coefficients ($P < .05$) were further assessed by specific organ within these body systems. The CD3 outcome variable was natural log-transformed to ensure the assumptions of linear regression were met; however, for one model (CD3 in air sac), the distribution of the residuals was not normal. Log transformation for Pax5 was unsuccessful at meeting all the assumptions of linear regression: while linearity was met in all 5 models, normality was met in all except 1 model (Pax5 in GI system), and homoscedasticity was met in all except 2 models (Pax5 in GI system and Pax5 in pancreas). These violations of the assumptions were likely caused by the relatively small dataset, which did not contain enough covariates to explain the outcome variables. Notwithstanding, these models have merit and were considered in our analysis.¹³ Significant ($P < .05$) regression coefficients describe a unit or percentage change in a specific immunophenotype proportion (ie, the proportion of cells reactive for either Pax5 or CD3) in a specific body system or organ compared to all the others. In order to determine if there was a sex predisposition, a Student's t test was conducted on the proportion of males versus females for cases that had sex specified in the report; 8 cases were excluded.

Table 1. Demographic Data for 38 Cases of Round Cell Neoplasia in Psittacine Birds.

| Case # | Genus | Species (common name) | Age (years) | Age category ^a | Sex |
|------------------------------------|----------------------|--------------------------|-------------|---------------------------|--------|
| B-cell lymphoma | | | | | |
| 1 | <i>Bolborhynchus</i> | Lineolated parakeet | 2 | Adult | Male |
| 2 | <i>Melopsittacus</i> | Budgerigar | 2 | Adult | Female |
| 3 | <i>Agapornis</i> | Lovebird | 2 | Juvenile | Male |
| 4 | <i>Nymphicus</i> | Cockatiel | 13 | Senior | Male |
| 5 | <i>Pionus</i> | Scaly-headed parrot | 13 | Senior | Female |
| 6 | <i>Pionus</i> | Bronze-winged pionus | 18 | Senior | Male |
| 7 | <i>Cacatua</i> | Moluccan cockatoo | 26 | Senior | Male |
| 8 | <i>Agapornis</i> | Lovebird | 15 | Senior | Male |
| 9 | <i>Nymphicus</i> | Cockatiel | 10 | Senior | Male |
| 10 | <i>Melopsittacus</i> | Budgerigar | N/A | N/A | Male |
| 11 | <i>Nymphicus</i> | Cockatiel | N/A | N/A | Female |
| 12 | <i>Nymphicus</i> | Cockatiel | N/A | N/A | Female |
| 13 | <i>Melopsittacus</i> | Budgerigar | N/A | N/A | Female |
| 14 | <i>Platycercus</i> | Rosella | 1 | Juvenile | Female |
| 15 | <i>Nymphicus</i> | Cockatiel | N/A | N/A | N/A |
| 16 | <i>Nymphicus</i> | Cockatiel | 15 | Senior | N/A |
| 17 | <i>Nymphicus</i> | Cockatiel | 11 | Senior | Female |
| 18 | <i>Melopsittacus</i> | Budgerigar | 1 | Juvenile | Female |
| 19 | <i>Bolborhynchus</i> | Lineolated parakeet | 3 | Adult | N/A |
| T-cell lymphoma | | | | | |
| 20 | <i>Agapornis</i> | Lovebird | 2 | Juvenile | Female |
| 21 | <i>Nymphicus</i> | Cockatiel | 21 | Senior | Male |
| 22 | <i>Pyrrhura</i> | Conure | 11 | Senior | N/A |
| T-cell lymphoma with MUM-1 | | | | | |
| 23 | <i>Nymphicus</i> | Cockatiel | N/A | N/A | Male |
| 24 | <i>Pyrrhura</i> | Green-cheeked conure | 19 | Senior | Female |
| 25 | <i>Melopsittacus</i> | Budgerigar | 3 | Adult | Female |
| Plasma cell tumor | | | | | |
| 26 | <i>Ara</i> | Yellow-collared macaw | 21 | Senior | Female |
| 27 | <i>Psittacula</i> | Indian ringneck parakeet | 1 | Juvenile | Female |
| 28 | <i>Nymphicus</i> | Cockatiel | 4 | Adult | Male |
| Double-reactive lymphoma | | | | | |
| 29 | <i>Amazona</i> | Amazon sp. | 12 | Adult | Male |
| 30 | <i>Nymphicus</i> | Cockatiel | 8 | Senior | N/A |
| 31 | <i>Nymphicus</i> | Cockatiel | 14 | Senior | Male |
| Non-B, non-T-cell neoplasia | | | | | |
| 32 | <i>Nymphicus</i> | Cockatiel | N/A | N/A | N/A |
| 33 | <i>Nymphicus</i> | Cockatiel | 7 | Adult | N/A |
| 34 | <i>Nymphicus</i> | Cockatiel | 1 | Juvenile | Female |
| 35 | <i>Nymphicus</i> | Cockatiel | N/A | N/A | Female |

(continued)

Table 1. (continued)

| Case # | Genus | Species (common name) | Age (years) | Age category ^a | Sex |
|---------------------|----------------------|-----------------------|-------------|---------------------------|--------|
| Undetermined | | | | | |
| 36 | <i>Cyanoramphus</i> | Kakariki | 5 | Adult | Male |
| 37 | <i>Melopsittacus</i> | Budgerigar | N/A | Adult | N/A |
| 38 | <i>Nymphicus</i> | Cockatiel | 5 | Adult | Female |

^aAge was categorized according to Gibson et al.⁸

Results

Signalment

Thirty-eight psittacine cases of round cell neoplasia, submitted to 3 North American institutions from 1999 to 2018, were included in the study. Round cell neoplasms were diagnosed in 13 psittacine genera, representing 14 species. The most common species were cockatiels (*Nymphicus hollandicus*; $n = 17$) and budgerigars (*Melopsittacus undulatus*; $n = 6$). Ages ranged from 8 months to 26 years (Table 1). Considering relative life spans, older birds were most frequently affected (senior [$n = 14$], adult [$n = 10$], juvenile [$n = 6$], and unknown [$n = 8$]). There was no observable difference in disease prevalence between sexes ($P = .72$, t test).

Tissues Affected

The 2 most common body systems affected were hepatic ($n = 29$) and gastrointestinal ($n = 29$; Table 2). Within these body systems, the most frequently affected organs were liver ($n = 29$), intestine ($n = 26$), kidney ($n = 20$), spleen ($n = 18$), pancreas ($n = 11$), proventriculus ($n = 11$), and ventriculus ($n = 7$; Suppl. Table S1). Tumors were most frequently multicentric with a median number of 5 (range 1–11) organs affected. Six cases had involvement of only a single organ: skin ($n = 3$), liver ($n = 2$), and brain ($n = 1$). Cutaneous cases involved the dermis and did not show epitheliotropism.

Histologic Features

Table 3 summarizes the histologic features of each case. Overall, tumors were formed by sheets of round cells with round to oval nuclei. Thirty-six of 38 cases (95%) had infiltrative growth pattern defined by presence of neoplastic cells dissecting between normal parenchymal cells, but 6 of these cases (16%) also showed expansile growth that was characterized in some areas by compression of surrounding tissues, amid the infiltrative pattern (Table 3). One case (case 11) showed only expansile growth pattern, where the neoplastic cells compressed the surrounding tissue without infiltration. Homogeneous populations of round cells were seen in 33 of 38 cases (87%). Nineteen of 38 cases (50%) were composed of large cells. Notable nucleoli were present in 24 cases (63%) with an

Table 2. Body Systems Affected by Round Cell Neoplasia in 38 Psittacine Birds.

| Type of neoplasia | Hepatic | Gastrointestinal | Urogenital | Lymphoid | Respiratory | Musculoskeletal | Nervous | Other |
|---|---------|------------------|------------|----------|-------------|-----------------|---------|-------|
| B-cell lymphoma (<i>n</i> = 19) | 15 | 19 | 16 | 9 | 3 | 2 | 1 | 4 |
| T-cell lymphoma (<i>n</i> = 3) | 2 | 1 | 1 | 1 | 1 | 0 | 0 | 2 |
| T-cell lymphoma with MUM-1 (<i>n</i> = 3) | 2 | 1 | 2 | 2 | 1 | 0 | 0 | 1 |
| Plasma cell tumor (<i>n</i> = 3) | 2 | 2 | 2 | 3 | 0 | 0 | 0 | 1 |
| Double-reactive lymphoma (<i>n</i> = 3) | 3 | 3 | 1 | 2 | 3 | 0 | 0 | 1 |
| Non-B, non-T-cell neoplasia (<i>n</i> = 4) | 3 | 2 | 0 | 2 | 0 | 0 | 0 | 1 |
| Unknown (<i>n</i> = 3) | 2 | 1 | 1 | 1 | 0 | 0 | 1 | 0 |
| Total | 29 | 29 | 23 | 20 | 8 | 2 | 2 | 10 |

average of 2 per cell. Prominent necrosis was present in 40% (*n* = 15) of cases. The mitotic count ranged from 0 to 107 per high-power field with an overall average of 21. Considering the 4 defined tiers of mitotic counts, there were 10 cases in the lowest tier (0–9.9 mitoses/field), 9 cases in tier 2 (10–19.9 mitoses/field), 12 cases in tier 3 (20–39.9 mitoses/field), and 4 cases in tier 4 (>40 mitoses/field). According to the original pathology reports, lymphoma was diagnosed in 34 cases, while round cell neoplasia not further specified was reported in the remaining 4 cases. These original diagnoses did not correlate with any distinct morphological patterns, therefore IHC was pursued to better resolve the diagnoses.

Immunohistochemistry of Normal Tissues

TMA cores from canine lymph node showed the expected patterns or reactivity for all 3 markers. In the chicken technical control and in the normal psittacine tissues, reactivity for all 3 markers was observed in the expected microanatomical locations for every species. Briefly, immunoreactivity for CD3 was finely granular and strongly cytoplasmic to membranous. Signal was present in most cells of the thymus, scattered cells throughout the bursa, and many cells in the periarteriolar lymphoid sheaths in the spleen; no reactivity was seen in the splenic follicles. Immunoreactivity for Pax5 was nuclear and was present in virtually all cells of the bursal and splenic follicles, rare cells in the thymus, and lymphocytes surrounding the sheathed penicillary capillaries in the spleen. Periarteriolar lymphoid sheaths showed very rare cells positive for Pax5. In some cases, non-B-cell reactivity for Pax5 was observed in epithelial cells lining the thyroid follicles, and some Purkinje cells in the brain. MUM-1 reactivity was mainly nuclear with occasional cytoplasmic signal and was localized in numerous cells in the bursal follicles.

Immunophenotypes of Lymphoid Neoplasia

Relative proportions of neoplastic cells immunoreactive for CD3, Pax5, and MUM-1 were used to categorize tumors into immunophenotypes (Figs. 1–6; Suppl. Table S2). A total of 17 cases were assessed by whole mount due to ambiguity of immunoreactivity or core loss. Overall, 4 patterns of immunoreactivity emerged (Fig. 1 and Suppl. Table S2). The first pattern was characterized by dominant immunoreactivity for a

single B- or T-cell marker in >70% of neoplastic cells, allowing for diagnosis of B-cell lymphoma, T-cell lymphoma, or plasma cell tumor. A second pattern showed double-reactivity for both B- and T-cell markers in >50% of cells simultaneously. These cases were reexamined using whole mounts to confirm double-reactivity across a larger tumor area and were diagnosed either as double-reactive lymphoma or T-cell lymphoma with MUM-1 reactivity. For MUM-1, concurrent reactivity with Pax5 was considered to indicate a B-cell immunophenotype. Cytoplasmic reactivity in addition to nuclear reactivity for MUM-1 was seen in 39% (*n* = 15) of neoplasia cases (Suppl. Table S2) and was considered specific reactivity. A third pattern showed no immunoreactivity in the neoplastic cells for any of the 3 markers, despite all internal controls being reactive. These cases were diagnosed as non-B, non-T-cell neoplasia. Last, a pattern of no reactivity was seen in 3 cases which lacked reactivity for all 3 markers in both the neoplastic cells and internal controls, preventing the determination of an immunophenotype. Lack of immunoreactivity in these 3 cases may have been due to autolysis or over-fixation.

The following paragraphs describe the characteristics of each of the 6 immunophenotypes. The relationships between final tumor diagnoses and demographic data, organ distribution, and histological features are summarized in Tables 1, 2, and 3, respectively.

Cases of B-cell lymphoma (*n* = 19) had a high proportion (average 89%) of Pax5-immunoreactive cells and very few (7%) CD3-positive cells (Figs. 1, 2; Suppl. Table S2). These tumors were, however, immunoreactive for MUM-1 in 16% of neoplastic cells on average, with 12 cases displaying reactivity for MUM-1 in >5% of neoplastic cells (Suppl. Table S2). All cases diagnosed as B-cell lymphoma were multicentric (median, 5 organs affected), all involved the gastrointestinal system (Table 3), and 17 of these 19 cases (90%) affected the intestine (Fig. 7) among other organs. B-cell lymphomas were histologically varied, without unifying features and spanning different cell sizes, nuclear features, and mitotic counts (Table 3). The most common size of the neoplastic cells was large (10/19 [53%]). The growth pattern was usually infiltrative (18/19 [95%]), or rarely expansile (4/19 [21%]). Seventeen of 19 cases of B-cell lymphoma were originally diagnosed as lymphoma, while the remaining 2 cases (cases 1 and 4) were described as round cell neoplasia not further specified.

Table 3. Histological Features of Different Immunophenotypes of Round Cell Neoplasia in 38 Psittacine Birds.

| Neoplasia category | Case | Number of organs affected | Infiltrative | Expansile ^a | Homogeneous ^b | Cell size ^c | Nucleus–cytoplasm ratio ^d | Prominent nucleoli | Number of nucleoli | Presence of necrosis ^e | Mitotic count ^f |
|-----------------------------|------|---------------------------|--------------|------------------------|--------------------------|------------------------|--------------------------------------|--------------------|--------------------|-----------------------------------|----------------------------|
| B-cell lymphoma | 1 | 7 | Yes | Yes | Yes | Medium | Medium | Yes | 2 | No | 41 |
| | 2 | 5 | Yes | No | Yes | Medium | Medium | Yes | 3 | No | 51 |
| | 3 | 4 | Yes | No | Yes | Large | Medium | No | 4 | No | 18 |
| | 4 | 9 | Yes | No | Yes | Large | Low | No | — ^g | No | 10 |
| | 5 | 11 | Yes | No | Yes | Large | Medium | Yes | 2 | No | 9 |
| | 6 | 5 | Yes | No | Yes | Large | Medium | Yes | 2 | No | 26 |
| | 7 | 8 | Yes | No | Yes | Medium | Medium | Yes | 1 | No | 36 |
| | 8 | 6 | Yes | No | Yes | Medium | Medium | Yes | 3 | No | 7 |
| | 9 | 3 | Yes | No | Yes | Small | High | No | — | Yes | 6 |
| | 10 | 7 | Yes | No | Yes | Small | High | Yes | 1 | Yes | 16 |
| | 11 | 6 | No | Yes | Yes | Large | Medium | Yes | 2 | Yes | 24 |
| | 12 | 3 | Yes | No | Yes | Medium | High | No | 1 | No | 28 |
| | 13 | 5 | Yes | No | Yes | Small | High | No | 1 | No | 19 |
| | 14 | 4 | Yes | Yes | Yes | Large | High | Yes | 1 | Yes | 27 |
| | 15 | 9 | Yes | No | Yes | Large | Medium | No | 1 | Yes | 19 |
| | 16 | 4 | Yes | No | Yes | Medium | High | Yes | 1 | No | 50 |
| | 17 | 2 | Yes | Yes | Yes | Large | Medium | Yes | 2 | Yes | 23 |
| | 18 | 5 | Yes | No | Yes | Large | High | Yes | 3 | No | 30 |
| | 19 | 8 | Yes | No | Yes | Large | Medium | Yes | 3 | Yes | 16 |
| T-cell lymphoma | 20 | 5 | Yes | No | Yes | Medium | High | Yes | 2 | Yes | 6 |
| | 21 | 5 | Yes | No | Yes | Small | Medium | No | — | No | — |
| | 22 | 1 | Yes | Yes | Yes | Small | High | Yes | 1 | No | 9 |
| T-cell lymphoma with MUM-1 | 23 | 3 | Yes | No | No | Large | Medium | Yes | 2 | Yes | 21 |
| | 24 | 1 | No | No | Yes | Large | Medium | Yes | 1 | No | 21 |
| | 25 | 7 | Yes | No | Yes | Medium | High | No | — | No | 29 |
| Plasma cell tumor | 26 | 9 | Yes | No | Yes | Large | Low | Yes | 1 | Yes | 2.7 |
| | 27 | 4 | Yes | No | Yes | Large | Medium | Yes | 1 | No | 11 |
| | 28 | 4 | Yes | No | No | Large | Low | No | — | Yes | 3 |
| Double-reactive lymphoma | 29 | 4 | Yes | No | Yes | Large | Medium | Yes | 2 | No | 9 |
| | 30 | 7 | Yes | No | Yes | Medium | Medium | Yes | 2 | Yes | 4 |
| | 31 | 3 | Yes | Yes | Yes | Medium | High | No | — | No | 33 |
| Non-B, non-T cell neoplasia | 32 | 5 | Yes | — | — | — | — | — | — | — | — |
| | 33 | 1 | Yes | No | Yes | Large | High | Yes | 2 | Yes | 107 |
| | 34 | 4 | Yes | No | No | Small | High | No | — | Yes | 14 |
| | 35 | 1 | Yes | No | Yes | Small | High | No | 1 | No | 28 |
| Undetermined | 36 | 1 | Yes | Yes | Yes | Large | Low | Yes | 3 | No | 16 |
| | 37 | 1 | Yes | — | — | — | — | — | — | — | — |
| | 38 | 6 | Yes | No | Yes | Large | Medium | Yes | 2 | Yes | 2 |

^a Defined as compression of the surrounding tissue.

^b Refers to the consistency in size of neoplastic cells and their nuclei.

^c Small (up to the size of one red blood cell), medium (1 to 1.5× the size of a red blood cell), or large (2× or more the size of a red blood cell).

^d Nucleus–cytoplasm volume ratio was defined relative to appearance of normal lymphocytes (high = normal).

^e Necrosis was defined as >20% of the tumor area.

^f Number of mitoses per 40× objective field fields, averaged from 3 fields (each field = 0.34 mm²).

^g —, Not assessed.

Six cases were consistent with a diagnosis of T-cell lymphoma based on >70% cellular immunoreactivity for CD3 (Figs. 1, 3, 4). Three T-cell lymphomas had 88% average immunoreactivity for CD3, and 4% and 3% immunoreactivity for Pax5 and MUM-1, respectively (Fig. 1, Suppl. Table S2). Three other cases were diagnosed as T-cell lymphoma with

MUM-1 reactivity (Fig. 4; Suppl. Table S2) based on reactivity for CD3 (93% of cells) and MUM-1 (57% of cells); these cases had minimal Pax5 immunoreactivity (3% of cells). One of these cases contained large, karyomegalic, often multinucleated cells, which were strongly immunoreactive for both CD3 and MUM-1 (Fig. 8). There were no clear patterns such

as anatomical distribution (Table 2) or cellular characteristics (Table 3) in either T-cell immunophenotype. One case of T-cell lymphoma with MUM-1 reactivity (case 24) was not infiltrative and was localized to the skin. All 6 cases were originally diagnosed as lymphoma.

Three cases were consistent with a diagnosis of plasma cell tumor based on 73% average cellular immunoreactivity for MUM-1, with little to no Pax5 (1%) or CD3 (4%) immunoreactivity (Figs. 1,5). However, internal controls for Pax5 could not be assessed in 2 of these cases presumably due to fixation artifact or autolysis. The 3 plasma cell tumors were composed of large, round cells with higher volume of cytoplasm compared to B-cell lymphoma in this study. One case (case 28) showed marked cellular atypia, with up to 3-fold anisokaryosis and anisocytosis. Two of 3 cases were originally diagnosed as lymphoma, while the remaining case (case 26) was originally diagnosed as round cell neoplasia.

Three cases were classified as double-reactive lymphoma, which were immunoreactive for both CD3 and Pax5 in an average of 80% and 73% of cells, respectively. These cases also showed MUM-1 immunoreactivity in an average of 33% of neoplastic cells (Figs. 1, 6). Features common to all 3 of these cases were the homogeneity of cell morphology and infiltrative nature of the tumors. All other demographic and histological features were variable (Tables 1–3). Severe effacement of the tissues with monomorphic populations of cells with high mitotic counts clearly suggested a neoplastic process; however, given the possibility of an infectious cause resulting in a mixed inflammatory reaction, PCR assays to detect avian *Coxiella* sp. and *Chlamydia psittaci* were performed and were negative. All 3 cases were originally diagnosed as lymphoma.

All 4 non-B, non-T-cell neoplasia cases in the present study were diagnosed in cockatiels and were defined by negligible reactivity for all 3 markers in the tumor area. Technical, genus-specific, and internal controls all reacted as expected, supporting the conclusion of lack of immunoreactivity in these tumors. One case of non-B, non-T-cell neoplasia (case 33) had the highest mitotic count in the cohort (107 mitoses per high-power [0.34 mm²] field; Suppl. Fig. S1). Two of these cases had localized involvement (ie, liver and skin). All 4 cases were originally diagnosed as lymphoma, with no obvious differential diagnoses.

Statistical Analysis

B- or T-cell immunophenotype was significantly associated with specific body systems or organs (Table 4) based on the immunoreactivity for either Pax5 or CD3. None of the regression coefficients from models using the percentage of MUM-1 immunoreactive cells were significant. Tumors affecting the gastrointestinal or urogenital systems had a higher percentage of cells immunoreactive for Pax5 (consistent with a diagnosis of B-cell lymphoma) compared to all other systems. Three cases were excluded in all Pax5 models because immunoreactivity could not be assessed. More specifically, within the gastrointestinal system, pancreas had the highest proportion of

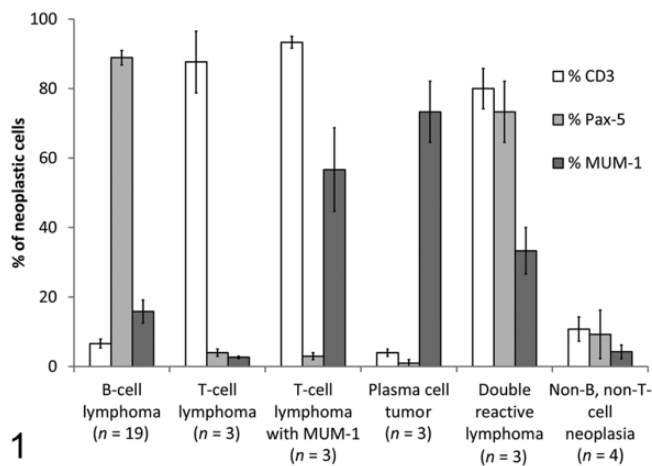


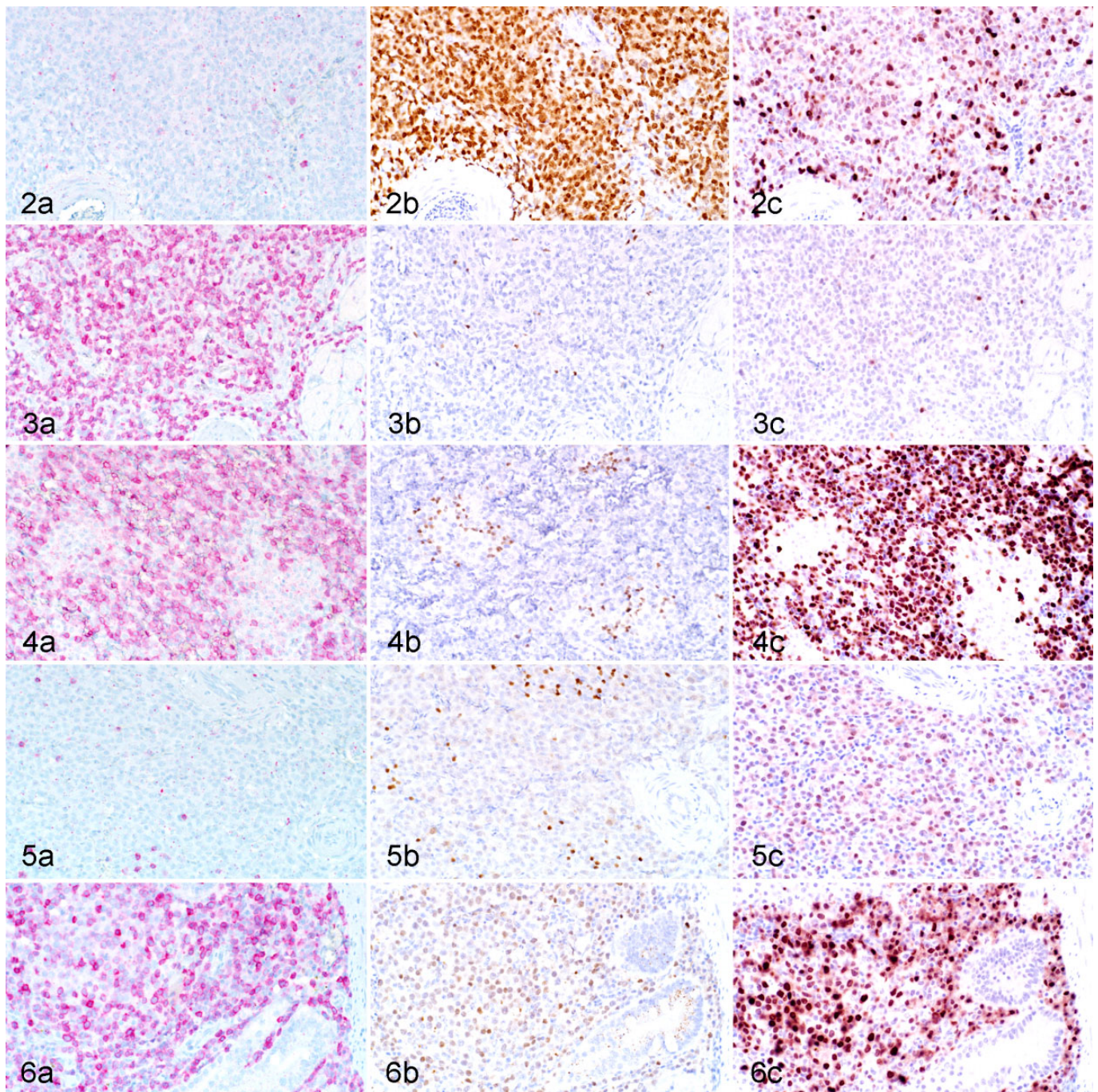
Figure 1. Percentage of cells that are immunoreactive for CD3, Pax5, and MUM-1 in 6 immunophenotypes of round cell neoplasms assessed in 38 psittacine birds. Mean \pm standard error. Three cases were excluded due to autolysis.

cells immunoreactive for Pax5 followed by intestine. Within the urogenital system, kidney had the highest proportion of cells immunoreactive for Pax5. Linear regression also showed that tumors affecting the respiratory system had a higher percentage of cells immunoreactive for CD3 (consistent with T-cell lymphoma), compared to all other systems. More specifically, this predilection was significantly higher for the air sac tissue.

Discussion

In the present study, the majority of round cell neoplasia cases in psittacine birds were consistent with lymphoma of B-cell origin, which had a predilection for the gastrointestinal and urogenital systems. Conversely, T-cell lymphoma tended to affect the respiratory system. In addition, plasma cell neoplasia, and novel immunophenotypic presentations of lymphoid neoplasia (ie, double-reactive lymphoma and T-cell lymphoma with MUM-1 reactivity) were also identified. This is the first report of such neoplasms in psittacine birds, which broadens the list of differential diagnoses for psittacine birds with lymphoid malignancies. Distinct cellular morphology was not observed between the different immunophenotypes, which highlights the importance of using immunohistochemistry to differentiate lymphoid neoplasms in these species.

The average mitotic count for all 38 cases was 21 per high-power field, with the most common count falling in tier 3, corresponding to 20 to 39.9 mitoses per high-power field (0.34 mm²). Mitotic count is often used to help determine the rate of proliferation and potential response to therapy (and thus prognosis) of lymphoma.⁴ In dogs, mitotic count ranges are well-defined as a metric to determine the grade; however, in the psittacine cases of this report, mitotic counts were comparatively higher, and different numerical categories were required for descriptive purposes.²⁵ Further studies are required to



Figures 2–6. Round cell neoplasms, psittacine birds. Columns “a,” “b,” and “c” show immunohistochemistry for CD3 (alkaline phosphatase chromogen, membranous labeling), Pax5 (alkaline phosphatase chromogen, nuclear labeling), and MUM-1 (NovaRed chromogen, nuclear and some cytoplasmic labeling), respectively. **Figure 2.** B-cell lymphoma, intestine, lineolated parakeet, case 1. There are rare cells with immunoreactivity for CD3 (a), while the majority shows strong immunoreactivity for Pax5 (b), and many cells are immunoreactive for MUM-1 (c). **Figure 3.** T-cell lymphoma, skin, green-cheeked conure, case 22. The majority of the neoplastic cells are immunoreactive for CD3 (a) and rare scattered cells are immunoreactive for Pax5 (b) and MUM-1 (c). **Figure 4.** T-cell lymphoma with MUM-1 reactivity, spleen, budgerigar, case 25. The majority of the cells are immunoreactive for CD3 (a), with only a few small cell aggregates immunoreactive for Pax5 (b). The majority of the cells are strongly immunoreactive for MUM-1 (c). **Figure 5.** Plasma cell tumor, spleen, Indian ring-necked parakeet, case 27. Scattered cells are immunoreactive for CD3 (a) and Pax5 (b), but the majority of the cells have mild immunoreactivity for MUM-1 (c). **Figure 6.** Double-reactive lymphoma, intestine, Amazon parrot, case 29. The majority of the cells show strong immunoreactivity for CD3 (a), light immunoreactivity for Pax5 (b), and strong to mild immunoreactivity for MUM-1 (c).

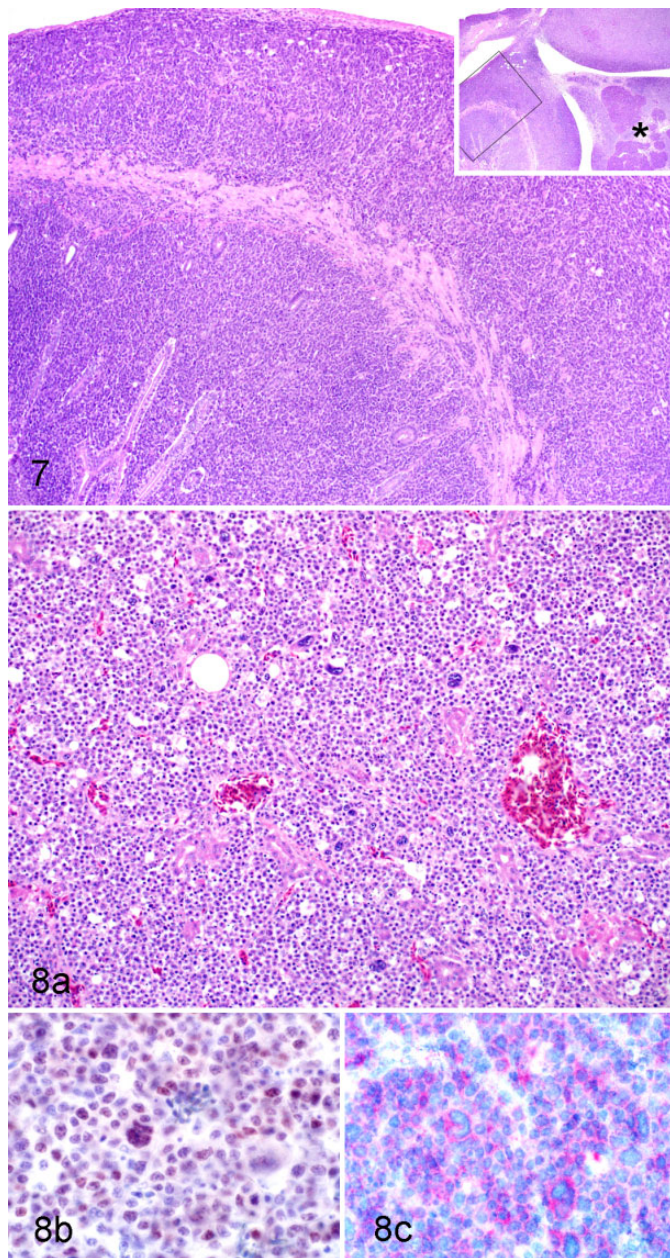


Figure 7. Infiltrative B-cell lymphoma, intestine, cockatiel, case 12. Neoplastic cells expand and efface the intestinal mucosa, submucosa, and muscularis. This neoplasm has a high proportion of Pax5 immunoreactive cells. Hematoxylin and eosin (HE). Inset: the neoplastic population transmurally effaces the intestine and extends to the adjacent pancreas (asterisk) and mesentery. HE. **Figure 8.** Infiltrative T-cell lymphoma with MUM-1 reactivity, liver, cockatiel, case 23. (a) There is marked anisocytosis and anisokaryosis and frequent multinucleate cells. HE. (b) Nuclear immunoreactivity for MUM-1. (c) Cytoplasmic to membranous immunoreactivity for CD3.

determine if prognostic differences exist between the different mitotic tiers evaluated in this study.

In addition to confirming the cross-reactivity of a commercial polyclonal antibody against human CD3 as a T-

lymphocyte marker in psittacines, as previously reported,²⁷ we also described for the first time the cross-reactivity of commercially available antibodies raised against human Pax5, a B-cell marker, and MUM-1, a plasma cell marker, in 14 psittacine species from 13 genera. Many commercially available antibodies are routinely used in IHC assays to diagnose various diseases in mammalian species; however, verification of cross-reactivity in new species requires additional testing on appropriate control tissues. Here we characterized immunoreactivity of these 3 markers in a group of psittacine birds utilizing normal lymphoid tissues as positive controls and demonstrated the utility of these lymphocyte markers in psittacine neoplastic tissues.

The CD3 marker identified 6 cases of T-cell lymphoma in the present study. Despite the additional reactivity of MUM-1 in 3 of these cases, a diagnosis of T-cell lymphoma remains the most likely because CD3 is very rarely ectopically expressed in non-T-lymphocytes, as described in the human literature.¹⁵ Furthermore, in humans MUM-1 expression has been reported in T-cell lymphomas and non-neoplastic activated T-cells,⁷ providing a biological precedent for the observed MUM-1 expression in psittacine T-cell lymphoma. In our cohort, additional cytoplasmic reactivity for the MUM-1 marker was often observed in cases of lymphoma in addition to the expected nuclear reactivity. This finding is similar to what was observed in congeneric normal lymphoid tissues, where nuclear and cytoplasmic MUM-1 reactivity was detected in B-cells and plasma cells identified based on the microanatomical location and cell morphology, thereby increasing our confidence that both nuclear and cytoplasmic expression in neoplastic cells represented specific reactivity of MUM-1.

In the 3 cases of double-reactive lymphoma, the concurrent reactivity of Pax5 and CD3, and to a lesser extent MUM-1, likely represents aberrant expression of the B-cell markers in lymphocytes of T-cell origin; however, cases of ectopic expression of CD3 in B-cell neoplasia have been documented in humans.¹⁵ Therefore, further testing to confirm the T-cell origin of these neoplasms is necessary. Notwithstanding, based on the patterns of reactivity in these 3 cases, other differential diagnoses included reactive inflammatory lesions such as those caused by *Chlamydia* or *Coxiella* spp. infection, or T-cell-rich B-cell lymphoma. Molecular testing (ie, PCR) ruled out infection with these 2 agents; however, other causes of lymphocytic inflammation are possible. T-cell-rich B-cell lymphoma is characterized by a neoplastic population of B cells infiltrated by >50% reactive T lymphocytes. This percentage can change with the progression of disease.^{1,19} Given the lack of morphologically distinct cell subpopulations clearly expressing either B-cell or T-cell markers, the possibility that double-reactivity could represent an artefact caused by an inflammatory infiltrate seems unlikely. However, further testing is required to confirm this interpretation.

Three cases in the cohort showed no reactivity to CD3, Pax5, or MUM-1 despite appropriate reactivity of the internal, congeneric, and technical controls. Differential diagnoses in

Table 4. Associations Between Anatomic Location of Round Cell Neoplasia and Percent of Immunoreactive Cells in 38 Psittacine Birds.

| IHC marker (Y) ^a | Category (X) ^b | Coefficients ^c | CI | t | P | R ² |
|-----------------------------|-------------------------------------|--|---|----------------------------|--------------------------------|----------------|
| Pax5 | Gastrointestinal^d | 67.5 (β₁) 2.3 (β₀) | 40.4 to 94.6 -22.0 to 26.5 | 5.06 0.19 | <.001 .849 | 0.44 |
| | Pancreas ^d | 46.4 (β ₁) 41.7 (β ₀) | 19.9 to 72.9 26.9 to 56.5 | 3.56 5.72 | .001 <.001 | 0.28 |
| | Intestine | 39.5 (β ₁) 28.1 (β ₀) | 10.7 to 68.3 3.8 to 52.4 | 2.79 2.35 | .009 .025 | 0.19 |
| | Urogenital | 33.3 (β₁) 35.4 (β₀) | 5.7 to 60.8 13.5 to 57.2 | 2.46 3.30 | .019 .002 | 0.15 |
| | Kidney | 30.2 (β ₁) 39.9 (β ₀) | 3.2 to 57.2 20.0 to 59.7 | 2.28 4.08 | .029 <.001 | 0.13 |
| | Respiratory | 1.3 (β₁) 2.0 (β₀)^e | 0.2 to 2.4 1.5 to 2.5 | 2.44 8.18 | .020 <.001 | 0.16 |
| ln(CD3) | Air sac ^d | 2.3 (β ₁) 2.2 (β ₀) | 0.3 to 4.3 1.7 to 2.6 | 2.34 9.59 | .025 <.001 | 0.17 |

Abbreviations: IHC, immunohistochemistry; CI, confidence interval; ln, natural log.

^aLinear variable describing the percent of cells (or natural log of the percent of cells) that are positive for a given marker (outcome variable).

^bBinary variable denoting presence or absence of involvement of anatomical category. Non-bolded categories are sub-categories of the preceding bolded body system.

^cRegression coefficients corresponding to the variables in the equation $Y = \beta_0 + \beta_1 X$.

^dDid not meet all the assumptions of linear regression (see text for details).

^eThe variable = coefficient when the X is zero.

these cases include non-B, non-T-cell lymphoma, histiocytic sarcoma, poorly granulated mast cell tumor, amelanotic melanoma, granular cell tumor, myelolipoma, and myeloproliferative disease, none of which have been reported in psittacine birds, with only histiocytic sarcoma being presumptively diagnosed in a great horned owl (*Bubo virginianus*).²⁰ One case report described an anaplastic, poorly pigmented melanoma in an umbrella cockatoo (*Cacatua alba*), which was confirmed by Fontana Masson stain.²³ The paucity of reports documenting other round cell neoplasia in psittacine birds is, at least in part, due to the lack of validated immunohistochemical markers that limits the characterization of these tumors. Markers commonly used to identify macrophages (ie, Iba-1 and KUL01) were not included in this study, as commercial antibodies against these antigens did not appear to cross-react with FFPE tissues in our cohort (data not shown). Non-B, non-T-cell lymphoma has been described in humans,¹⁰ and given the lymphoid morphology of the cases in this group, this diagnosis remains possible.

The anatomic distribution of round cell tumors in the present study was variable; localized involvement was observed in 6 cases, 2 of which were consistent with T-cell lymphoma affecting exclusively the dermis/subcutis; however, one case (case 33) did not have a comprehensive list of tissues to be assessed and distribution to other organs could not be confirmed. Cutaneous lymphoma has been reported in a double yellow-headed Amazon parrot (*Amazona ochrocephala oratrix*); however, spleen and bone marrow were also affected.² In our cohort, other localized neoplasms had a non-B, non-T-cell, or

undetermined immunophenotype, suggesting that localization in psittacine birds may indicate non-lymphoid round cell neoplasia and requires further diagnostic workup.

The use of TMA technology in the present study allowed for direct comparisons among cases by limiting the between-sample variation, to better assess case-specific differences in the nature of the neoplasms, fixation artifact, and species characteristics. Additionally, the use of TMAs facilitated the efficient assessment of reactivity for round cell markers in psittacines. Previous studies suggest that cores taken from lymphoid neoplasms are sufficient to characterize immunophenotype,⁹ and this proved true in more than half of the cases in the present study. However, further characterization was deemed necessary in 17 cases due to unexpected expression patterns or core loss.

This study described round cell neoplasia of psittacine birds including morphologic and immunophenotypic characterization, and represents a benchmark for future studies that could lead to more accurate diagnostic algorithms, as well as development of prognostic studies and effective treatment protocols for these diseases.

Acknowledgements

We thank all the institutions who contributed cases to this research. Specifically, the University of Montreal through Dr Sonia Chenier. We also are grateful to the clinics that granted permission for inclusion of case material submitted to Northwest ZooPath: Lion Country Safari (Loxahatchee, FL), Forth Worth Zoo (Fort Worth, TX), Woodland Park Zoo (Seattle, WA), Windcrest Animal Hospital (Wilmington,

DE), All Creatures Animal Hospital (East Amherst, NY), Extra Care Animal Hospital (Davie, FL), Brook-Falls Veterinary Hospital & Exotic Care, Inc (Brookfield, WI), Chicago Exotics (Skokie, IL), Volunteer Veterinary Clinic (Hendersonville, TN), Gulf Coast Avian & Exotics (Houston, TX), Amwell Bird Hospital (Hillsborough, NJ), Sno-Wood Veterinary Hospital (Woodinville, WA), Carolina Veterinary Specialists (Huntersville, NC), Caldwell Zoo (Tyler, TX), Bird & Exotic Specialty (Norton, OH), Chippens Hill Veterinary Hospital (Bristol, CT), Animal Health Clinic (Jupiter, FL), Old Country Animal Clinic (Plainview, NY), and Coventry Animal Hospital (Coventry, RI). We also thank the pathologists and graduate students at the University of Guelph who originally diagnosed these cases, especially Drs D. A. Smith, M. Brash, and E. Martin.





Declaration of Conflicting Interests

The author(s) declared no potential conflicts of interest with respect to the research, authorship, and/or publication of this article.

Funding

The author(s) disclosed receipt of the following financial support for the research, authorship, and/or publication of this article: We acknowledge the Ontario Veterinary College Pet Trust for funding the project (Grant 052654).

ORCID iD

Daniel J. Gibson  <https://orcid.org/0000-0002-0614-8298>
 Hugues Beaufrère  <https://orcid.org/0000-0002-3612-5548>
 Csaba Varga  <https://orcid.org/0000-0003-2751-3677>
 Leonardo Susta  <https://orcid.org/0000-0002-4578-6145>

References

- Aquino SM, Hamor RE, Valli VE, et al. Progression of an orbital T-cell rich B-cell lymphoma to a B-cell lymphoma in a dog. *Vet Pathol.* 2000;**37**(5):465–469.
- Burgos-Rodríguez AG, Garner M, Ritzman TK, et al. Cutaneous lymphosarcoma in a double yellow-headed Amazon parrot (*Amazona ochrocephala oratrix*). *J Avian Med Surg.* 2007;**21**(4):283–289.
- Calnek BW. Pathogenesis of Marek's disease virus infection. In: Hirai K, ed. *Marek's Disease*. Springer-Verlag; 2001:25–55.
- Carrasco V, Rodríguez-Bertos A, Rodríguez-Franco F, et al. Distinguishing intestinal lymphoma from inflammatory bowel disease in canine duodenal endoscopic biopsy samples. *Vet Pathol.* 2015;**52**(4):668–675.
- Coleman C. Lymphoid neoplasia in pet birds: a review. *J Avian Med Surg.* 1995;**9**(1):3–7.
- Cushing TLL, Schat KAA, States SLL, et al. Characterization of the host response in systemic isosporosis (atoxoplasmosis) in a colony of captive American goldfinches (*Spinus tristis*) and house sparrows (*Passer domesticus*). *Vet Pathol.* 2011;**48**(5):985–992.
- Falini B, Fizzotti M, Pucciarini A, et al. A monoclonal antibody (MUM1p) detects expression of the MUM1/IRF4 protein in a subset of germinal center B cells, plasma cells, and activated T cells. *Blood.* 2000;**95**(6):2084–2092.
- Gibson DJ, Nemeth NM, Beaufrère H, et al. Captive psittacine birds in Ontario, Canada: a 19-year retrospective study of the causes of morbidity and mortality. *J Comp Pathol.* 2019;**171**:38–52.
- Hammer AS, Williams B, Dietz HH, et al. High-throughput immunophenotyping of 43 ferret lymphomas using tissue microarray technology. *Vet Pathol.* 2007;**44**(2):196–203.
- Karube K, Ohshima K, Tsuchiya T, et al. Non-B, non-T neoplasms with lymphoblast morphology: further clarification and classification. *Am J Surg Pathol.* 2003;**27**(10):1366–1374.
- Kuhns MS, Davis MM, Garcia KC. Deconstructing the form and function of the TCR/CD3 complex. *Immunity.* 2006;**24**(2):133–139.
- Le K, Beaufrère H, Brouwer E, et al. Retro-orbital and disseminated B-cell lymphoma in a yellow-collared macaw (*Primolius auricollis*). *Can Vet J.* 2017;**58**(7):707–712.
- Lumley T, Diehr P, Emerson S, et al. The importance of the normality assumption in large public health data sets. *Annu Rev Public Health.* 2002;**23**:151–169.
- Nemeth NM, Gonzalez-Astudillo V, Oesterle PT, et al. A 5-year retrospective review of avian diseases diagnosed at the department of pathology, University of Georgia. *J Comp Pathol.* 2016;**155**(2–3):105–120.
- Oliveira JL, Grogg KL, Macon WR, et al. Clinicopathologic features of B-cell lineage neoplasms with aberrant expression of CD3: a study of 21 cases. *Am J Surg Pathol.* 2012;**36**(9):1364–1370.
- Parmentier S, Fischer D, Wüst E, et al. Generalized lymphoma with a displacing mass in the orbital cavity of a Pacific parrotlet (*Forpus coelestis*). *Comp Clin Pathol.* 2017;**26**:1389–1394.
- Rivera S, McClearn JR, Reavill DR. Treatment of nonepitheliotropic cutaneous B-cell lymphoma in an umbrella cockatoo (*Cacatua alba*). *J Avian Med Surg.* 2009;**23**(4):294–302.
- Robat CS, Ammersbach M, Mans C. Avian oncology: diseases, diagnostics, and therapeutics. *Vet Clin North Am Exot Anim Pract.* 2017;**20**(1):57–86.
- Rodríguez J, Pugh WC, Cabanillas F. T-cell-rich B-cell lymphoma. *Blood.* 1993;**82**(5):1586–1589.
- Sacré BJ, Oppenheim YC, Steinberg H, et al. Presumptive histiocytic sarcoma in a great horned owl (*Bubo virginianus*). *J Zoo Wild Med.* 2014;**23**:113–121.
- Sinclair KM, Hawkins MG, Wright L, et al. Chronic T-cell lymphocytic leukemia in a black swan (*Cygnus atratus*): diagnosis, treatment, and pathology. *J Avian Med Surg.* 2015;**29**(4):326–335.
- Souza MJ, Newman SJ, Greenacre CB, et al. Diffuse intestinal T-cell lymphosarcoma in a yellow-naped Amazon parrot (*Amazona ochrocephala auropaliiata*). *J Vet Diagn Invest.* 2008;**20**(5):656–660.
- Stern AW, Lamm CG. Malignant melanoma of the subcutaneous tissues in an umbrella cockatoo (*Cacatua alba*). *J Avian Med Surg.* 2009;**23**(4):303–306.
- Ushio N, Watanabe KI, Chambers JK, et al. *Sarcocystis calchasi* encephalitis in a rock pigeon. *J Vet Med Sci.* 2015;**77**(11):1523–1526.
- Valli VE, Myint M, Barthel A, et al. Classification of canine malignant lymphomas according to the World Health Organization criteria. *Vet Pathol.* 2011;**48**(1):198–211.
- Willmann M, Müllauer L, Guija de Arespacochaga A, et al. Pax5 immunostaining in paraffin-embedded sections of canine non-Hodgkin lymphoma: a novel canine pan pre-B- and B-cell marker. *Vet Immunol Immunopathol.* 2009;**128**(4):359–365.
- Zehnder A, Graham J, Reavill D, et al. Neoplastic diseases in avian species. In: Speer BL, ed. *Current Therapy in Avian Medicine and Surgery*. Elsevier; 2016:107–141.